Long Baseline Neutrino Oscillation Experiments

Mark Thomson
Cavendish Laboratory
Department of Physics
JJ Thomson Avenue
Cambridge, CB3 0HE
United Kingdom

1 Introduction

In the last ten years the study of the quantum mechanical effect of neutrino oscillations, which arises due to the mixing of the weak eigenstates $\{\nu_e, \nu_\mu, \nu_\tau\}$ and the mass eigenstates $\{\nu_1, \nu_2, \nu_3\}$, has revolutionised our understanding of neutrinos. Until recently, this understanding was dominated by experimental observations of atmospheric [1, 2, 3] and solar neutrino [4, 5, 6] oscillations. These measurements have been of great importance. However, the use of naturally occuring neutrino sources is not sufficient to determine fully the flavour mixing parameters in the neutrino sector. For this reason, many of the current and next generation of neutrino experiments are based on high intensity accelerator generated neutrino beams. The first generation of these long-baseline (LBL) neutrino oscillation experiments, K2K, MINOS and CNGS, are the main subject of this review. The next generation of LBL experiments, T2K and NOνA, are also discussed.

2 Theoretical Background

For two neutrino weak eigenstates $\{\nu_\alpha, \nu_\beta\}$ related to two mass eigenstates $\{\nu_i, \nu_j\}$, by a single mixing angle θ_{ij}, it is simple to show that the survival probability of a neutrino of energy E_ν and flavour α after propagating a distance L through the vacuum is

$$P(\nu_\alpha \to \nu_\alpha) \;=\; 1 - \sin^2 2\theta_{ij} \sin^2\left(\frac{1.27\Delta m^2_{ji}(\mathrm{eV}^2)L(\mathrm{km})}{E_\nu(\mathrm{GeV})}\right), \qquad (1)$$

where Δm^2_{ji} is the difference of the squares of the neutrino masses, $m_j^2 - m_i^2$. From the Z lineshape measurements at LEP [7], we know that there are exactly three active flavours of neutrinos (assuming $m_\nu < m_\mathrm{Z}/2$) and it is straightforward to extend the two flavour treatment of neutrino oscillations to three flavours. Assuming neutrinos are Dirac particles, the single mixing angle of Equation 1 is replaced by the three mixing angles $\{\theta_{12}, \theta_{13}$ and $\theta_{23}\}$, and a phase angle, δ. The relation between the weak and mass eigenstates is described by the PMNS matrix [8, 9] which can be expressed in the convenient form

$$U_{\rm PMNS} = \begin{pmatrix} 1 & 0 & 0 \\ 0 & c_{23} & s_{23} \\ 0 & -s_{23} & c_{23} \end{pmatrix} \begin{pmatrix} c_{13} & 0 & s_{13}e^{i\delta} \\ 0 & 1 & 0 \\ -s_{13}e^{i\delta} & 0 & c_{13} \end{pmatrix} \begin{pmatrix} c_{12} & s_{12} & 0 \\ -s_{12} & c_{12} & 0 \\ 0 & 0 & 1 \end{pmatrix}, \tag{2}$$

where $c_{ij} = \cos\theta_{ij}$ and $s_{ij} = \sin\theta_{ij}$. Hence the phenomenology of neutrino oscillations is described by four angles $\{\theta_{12}, \theta_{13}, \theta_{23}$ and $\delta\}$ and two independent mass-squared differences, Δm^2_{21} and Δm^2_{32}. A non-zero value for δ leads to CP violation in the lepton sector provided $\sin\theta_{13}$ is also non-zero.

2.1 Atmospheric, Solar and Reactor Neutrino Data

In the limit that $|\Delta m^2_{32}| \gg |\Delta m^2_{21}|$, for many experiments it is a reasonable approximation to reduce the full three flavour treatment of neutrino oscillations to the two flavour form of Equation 1. In the treatment of solar neutrino data matter effects have to be included. In the two-flavour approximation, solar neutrino data from SNO [6] and reactor neutrino data from KamLAND [10] determine the relevant solar Δm^2 scale to be $|\Delta m^2_{\odot}| = (7.59 \pm 0.21) \times 10^{-5}\,\mathrm{eV}^2$ and $\tan^2\theta_{\odot} = 0.47^{+0.06}_{-0.05}$. In the two-flavour approximation, the atmospheric neutrino data [1, 2, 3] yield $|\Delta m^2_{\rm atm.}| \approx 2.5\times 10^{-3}\,\mathrm{eV}^2$ and the mixing angle $\sin^2 2\theta_{\rm atm.} \approx 1$. These results can be placed in the context of three neutrino flavours. The mass eigenstates dominating solar neutrino oscillations are defined to be ν_1 and ν_2, where $m_1 < m_2$. Hence, the solar neutrino data determine Δm^2_{21} and $\tan^2\theta_{12}$. The atmospheric neutrino data place a lower limit on $\sin^2 2\theta_{23} > 0.95$ (90 % C.L.) and provide a measurement of $|\Delta m^2_{32}|$. The data do not determine the mass hierarchy, *i.e.* whether $m_3 > m_2$ or $m_3 < m_2$. In addition, the CHOOZ [11] reactor data constrains $\sin^2 2\theta_{13} < 0.15$ (the exact value depends on $|\Delta m^2_{32}|$).

In summary, solar and atmospheric neutrino experiments have provided measurements of Δm^2_{21}, $|\Delta m^2_{32}|$ and θ_{12}. Currently there is no experimental constraint on the phase δ, only a lower limit on $\sin^2 2\theta_{23}$ and an upper limit on $|\theta_{13}|$.

3 Long-baseline Neutrino Oscillation Experiments

LBL experiments use intense ν_μ beams to investigate neutrino oscillations. The main parameters of the past (K2K), present (MINOS, OPERA), and future (T2K, NOνA) LBL experiments are summarised in Table 1. Each of the experiments has specific physics goals: K2K was designed to verify the atmospheric neutrino oscillation results from SK; MINOS was designed to perform precise measurements of the atmospheric oscillation parameters and may have sensitivity to θ_{13}; OPERA is designed to make the first observation of ν_τ appearance in $\nu_\mu \leftrightarrow \nu_\tau$ oscillations; T2K is designed for the observation of $\nu_\mu \leftrightarrow \nu_e$ and the measurement of θ_{13} (depending on the value of θ_{13}, phase II of the T2K experiment may have sensitivity to δ); NOνA has similar goals to T2K but, due to the longer baseline, may also determine of the mass hierarchy. Before discussing these five experiments it is first worth considering how the intense neutrino beams are produced.

Experiment	Operational	Peak E_ν	Baseline	Detector
K2K	1999 – 2004	1 GeV	250 km	Water Čerenkov
NuMI/MINOS	2005 – 2011(?)	3 GeV	735 km	Steel/Scintillator
CNGS/OPERA	2008–	17 GeV	732 km	Emulsion
T2K	2010–	0.7 GeV	295 km	Water Čerenkov
NOνA	2012(?)–	1.8 GeV	810 km	Liquid Scintillator

Table 1: Summary of the main parameters of past, present and future long-baseline neutrino oscillations experiments. It should be noted that at this time the schedule for NOνA is uncertain.

3.1 Neutrino Beams

All long-baseline experiments adopt the same basic approach to produce a collimated ν_μ beam. Firstly, an intense beam of protons is focused onto a target. The target is designed to maximise the production of secondary hadrons whilst minimising the number of secondary interactions. The secondary particles produced from the target are then focused by magnetic horns, shown schematically in Figure 1. Neutrino horns (typically) consist of shaped inner conductors joined to a cylindrical outer conductor. In coincidence with the beam spill, the horns are pulsed with large current, $O(100\,\text{kA})$, which circulates via the inner and outer conductors. By a simple application of Ampere's law it can be seen that this generates a large magnetic field proportional to $1/r$ in the region between the inner and outer conductors. Because particles at larger angles to the primary beam axis traverse more of the region between the conductors where the field exists, they receive a larger transverse momentum kick. In this way, positive particles, such as π^+ and K^+, tend to be focused and negative particles are defocused. Different experiments use one, two or three horns to achieve the optimal focusing for the desired neutrino beam energy. The focused particles, predominantly π^+, then traverse a long (hundreds of metres) decay region where neutrinos are produced from $\pi^+ \rightarrow \mu^+\nu_\mu$ decays. Muon neutrinos are also produced in $K^+ \to \mu^+\nu_\mu$ decays. The $\nu_e/\overline{\nu}_e$ contamination in the beam, which arises from μ^+ and K^0 decays, is typically of order 1 %.

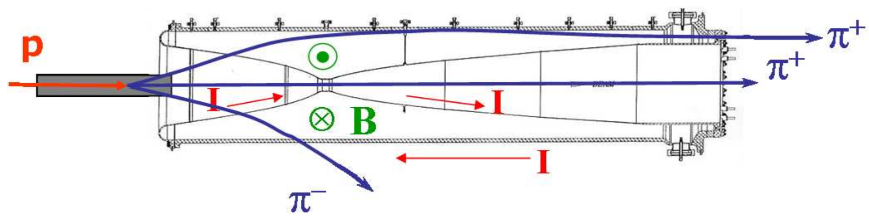

Figure 1: A schematic diagram showing the focusing (de-focusing) of secondary π^+ (π^-) by the magnetic field in between the inner and outer conductors of a neutrino horn (in this case MINOS horn 1).

3.2 Interaction Rate Uncertainties

It is important to note that it is not possible to predict the neutrino flux and energy spectrum with high accuracy since the process of hadron production from the target is not well modelled in the Monte Carlo simulations. This reflects the lack of hadron production data in the relevant kinematic regions. This situation should improve to some extent with the publication of MIPP data [12]. There are also significant uncertainties in low energy neutrino cross sections and interaction kinematics. As a result, the expected neutrino interaction rate in a LBL experiment is a combination of the imperfectly modelled beam spectrum and the imperfectly modelled neutrino cross sections. Consequently measurement of the unoscillated beam, *i.e.* in a near detector close to production, is essential to accurately predict the expectation at the far detector.

3.3 K2K

The KEK to Kamioka (K2K) experiment, which took data from 1999 until 2004, was the first LBL neutrino oscillation experiment. The main goal was to confirm the Super-Kamiokande atmospheric neutrino observations in a controlled beam experiment. An almost pure muon neutrino beam was created from 12 GeV proton synchrotron (KEK-PS) with a typical intensity of about 5×10^{12} protons per pulse. The beam was directed towards the Super-Kamiokande (SK) water Čerenkov detector located 250 km away. Two near detectors were employed; a 1 kton water Čerenkov detector and fine-grained detector system consisting of a scintillating-fibre/water target tracker) and a lead-glass calorimeter which was upgraded to a totally active fine-segmented scintillator tracker (Sci-Bar). The neutrino beam direction and unoscillated energy spectrum were measured by the near detector system. K2K accumulated 9.2×10^{19} protons-on-target (PoT) of data for the physics analysis. A total of 112 neutrino beam induced events were observed in 22.5 kton fiducial volume of the SK detector, while $158.1^{+9.2}_{-8.6}$ were expected without oscillation [13].

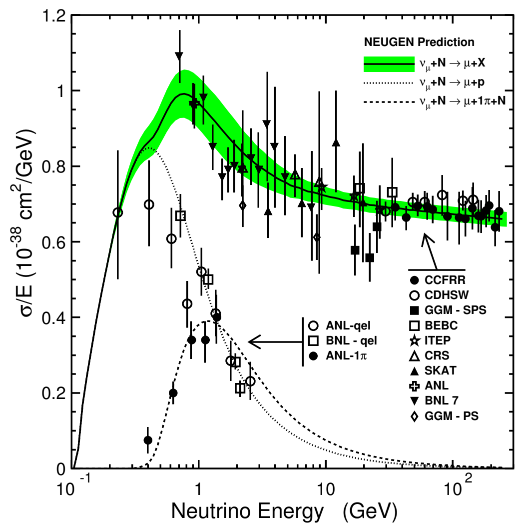

Figure 2: Neutrino cross-section data [14] compared to the prediction from the Neugen program [15]. The dotted curve indicates the quasi-elastic ($\nu_\mu + \mathrm{n} \rightarrow \mu^- + \mathrm{p}$) contribution and the dashed curve indicates the resonance contribution with a single pion in the final state, (*e.g.* $\nu_\mu + \mathrm{n} \rightarrow \mu^- + \Delta^+ \rightarrow \mu^- + \pi^+ + \mathrm{n}$) contribution. At higher energies deep inelastic scattering dominates. Plot taken from [16].

For the K2K baseline and the measured value of $\Delta m^2_{\mathrm{atm}}$, the $\nu_\mu \rightarrow \nu_\mu$ oscillation minimum is expected at approximately 0.6 GeV. For this energy, the neutrino cross section (see Figure 2) is dominated by quasi-elastic scattering, $\nu_\mu + \mathrm{n} \rightarrow \mu^- + \mathrm{p}$, resulting in a single Čerenkov ring from the relativistic muon. The next most important process is resonance production, *e.g.* $\nu_\mu + \mathrm{n} \rightarrow \mu^- + \Delta^+ \rightarrow \mu^- + \mathrm{n} + \pi^+$, resulting in Čerenkov two rings. For quasi-elastic interactions, the event kinematics ($x = 1$) enable the neutrino energy to be determined from the measured energy and direction of the muon alone,

$$E_\nu^{\mathrm{rec}} = \frac{m_N E_\mu - m_\mu^2/2}{m_N - E_\mu + p_\mu \cos\theta_\mu}, \tag{3}$$

where E_μ and p_μ are the muon energy and momentum, and $\cos\theta_\mu$ is the muon scattering angle with respect to the beam direction. Note that in Equation 3 the Fermi motion of the struck nucleon has been neglected. To measure the effect of neutrino oscillations on the neutrino energy spectrum, quasi-elastic interaction events are selected by requiring a single reconstructed Čerenkov ring consistent with originating from a muon. The neutrino energy spectrum from 58 single-ring muon-like events is shown in Figure 3a. A distortion of the energy spectrum is observed, consistent with neutrino oscillations. Since θ_{13} is known to be small, Equation 1 is used to fit the data. The allowed oscillation parameter region from the measurements of the number of events and energy spectrum is shown in Figure 3b, along with the SK atmospheric neutrino results. The K2K results discriminated against the null oscillation hypothesis at the 4.3σ level and provided verification of $\Delta m^2_{\rm atm}$ obtained from SK.

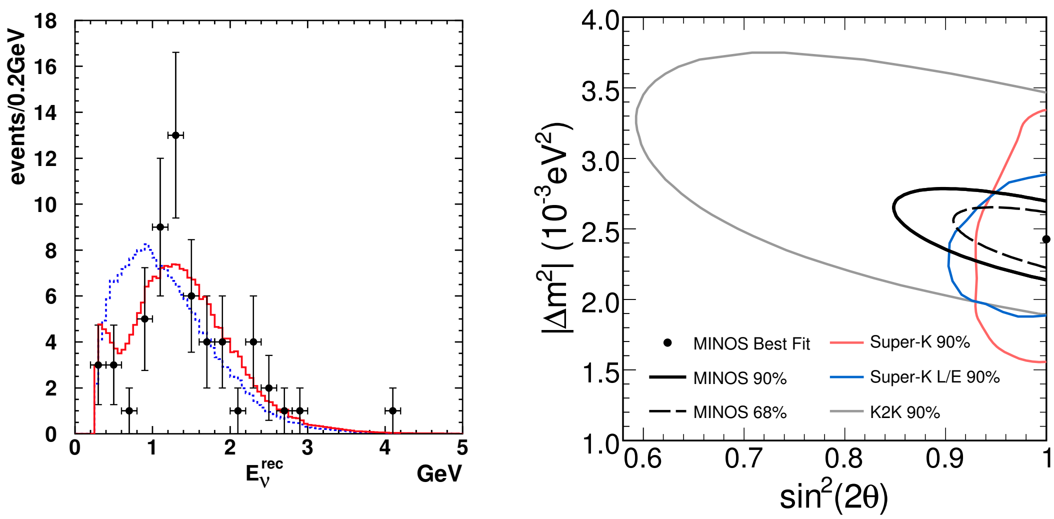

Figure 3: **a)** Energy spectrum for the observed 58 single-ring muon-like events from the K2K experiment. The solid red line is the expectation without oscillations and the dashed blue line shows the expectation for the best fit oscillation parameters. In both cases the expected spectra are normalised to the data. Taken from [13]. **b)** A comparison of 90 % C.L. contours in $|\Delta m^2|$ and $\sin^2 2\theta$ from two-flavour fits to atmospheric neutrino (SK) and LBL (K2K and MINOS) data. Taken from [18].

3.4 MINOS

Whilst K2K provided impressive confirmation of the SK atmospheric neutrino results, the measurements of the oscillation parameters were statistically limited. The main goal of the MINOS experiment [17] is the precise measurement of $|\Delta m^2_{32}|$ and discrimination against alternative hypotheses such as neutrino decay and quantum decoherence. To achieve this, the NuMI beam is an order of magniude more intense than that of the K2K experiment. In addition, MINOS may have sensitivity to θ_{13} through sub-dominant $\nu_\mu \to \nu_e$ oscillations and may be able to further constrain θ_{23}.

The MINOS experiment has been taking data from the NuMI beam at Fermilab (FNAL) since 2005. The neutrino beam is produced using 120 GeV protons from the FNAL Main Injector incident on a graphite target. Pions are focused using two magnetic horns. The neutrino energy spectrum can be changed by adjusting either the horn current or the position of the target relative to the horns. The majority of the MINOS data has been taken in the lowest energy configuration (LE), for which the peak of the neutrino energy spectrum is at 3.3 GeV. The typical beam intensity is $\sim 2.5 \times 10^{13}$ protons per pulse with a 2.4 s cycle time. By the end of 2008 MINOS had recorded 6×10^{20} PoT. The results reported here are based on an exposure of 3.4×10^{20} PoT [18].

For the MINOS baseline of 735 km, the $\nu_\mu \to \nu_\mu$ oscillation minimum occurs at approximately 1.6 GeV (higher than for K2K). Hence for the MINOS experiment quasi-elastic, resonance and deep-inelastic scattering interactions all play a role (see Figure 2), and it is no longer possible to reconstruct the neutrino energy from the reconstructed muon alone. The MINOS detectors are magnetised steel-scintillator sampling calorimeters with alternating layers of 2.54 cm thick steel and 1 cm thick plastic scintillator strips. The detector is able measure the muon momentum (from curvature or range) and the energy of the recoiling hadronic system in charged-current (CC) interactions, ν_μ+Fe $\to \mu^-$+X. The 5.4 kton MINOS far detector (FD) is located in the Soudan Underground Laboratory 735 km away from the NuMI target. The 0.98 kton Near Detector (ND) is located 1.04 km from target. The ND and FD use the same basic detector technology and are functionally very similar. By comparing the neutrino energy spectrum in the near and far detectors systematic uncertainties associated with neutrino beam flux, interaction cross sections and detector response largely cancel.

Candidate ν_μ CC interaction events are selected using a multivariate technique using variables related to the (muon) track properties. The neutrino energy is reconstructed as the sum of the muon track momentum and hadronic shower energies. The measured near detector neutrino energy spectrum is used to predict the unoscillated spectrum at the far detector. However, from the point of view of the decaying mesons which produce the neutrino beam the near detector subtends a much larger solid angle than the far detector. Consequently, even in the absence of neutrino oscillations, the near and far detector energy spectra are not identical. This is corrected for by extrapolating the measured neutrino energy spectrum in the near detector to that in the far detector using the Beam Matrix method [16].

For LE beam data, 730 CC ν_μ events are observed in the FD compared to the unoscillated expectation of 936 ± 53. The energy spectrum is shown in Figure 4a. A fit to the data using Equation 1 gives $|\Delta m^2| = (2.43 \pm 0.13) \times 10^{-3}\,\mathrm{eV}^2$ and $\sin^2 2\theta > 0.95$ at the 68 % C.L. The fit $\chi^2 = 90$ for 97 degrees of freedom. The 68 % C.L. and 90 % C.L. contours are shown in Figure 3b. The ratio of the observed FD energy spectra to that expected in the absence of neutrino oscillations is shown in Figure 4b. Here the data are also compared to fits using alternative models that have been proposed to explain the disappearance of neutrinos in flight, namely, the decay of neutrinos to lighter particles (Equation 13 of [19]) and the decoherence of the neutrino quantum-mechanical wave packet (Equation 5 of [20]). These alternative models are disfavoured with respect to the oscillation hypothesis at the 3.7 and 5.7 standard deviation level.

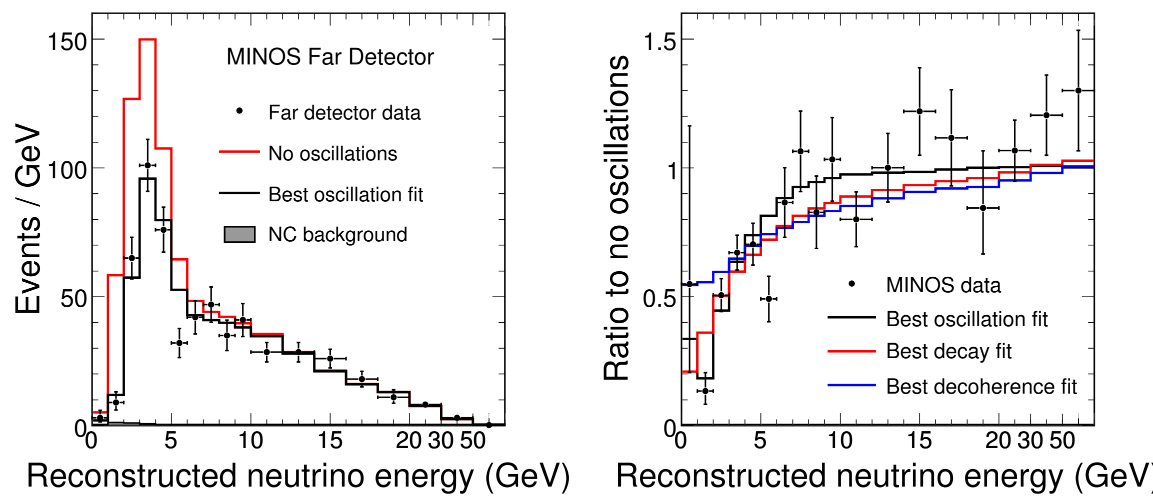

Figure 4: **a)** Reconstucted neutrino energy spectrum for selected ν_μ CC interactions in the MINOS FD. The data are compared to the unoscillated expectation and the best fit. **b)** The ratio of the observed energy spectrum of selecred ν_μ CC interactions in the MINOS FD to the expected spectrum in the absence of oscillations (null hypothesis). The data are compared to the best fit and also to the hypotheses of neutrino decay and neutrino decoherence. Both plots taken from [18].

MINOS may have sensitivity to sub-dominant $\nu_\mu \to \nu_e$ oscillations. Because θ_{13} is known to be small, the event rate is low (at most ~20 events are expected in the current data sample). The measurement of this small signal is complicated by the large potential background from neutral current interactions with one or more π^0s in the final state; the decays of π^0s produce electromagnetic (EM) showers which can mimic the signal, *i.e.* an EM shower from the electron in $\nu_e + \text{Fe} \to \text{e}^- + \text{X}$. Furthermore, the coarse sampling of the MINOS detector is far from optimal for identifying electrons from ν_e CC interactions. Nevertheless, the MINOS collaboration has developed sophisticated event identification algorithms and techniques to determine the expected background from the near detector data. First results based on 3.25×10^{20} PoT are expected early in 2009 with preliminary expected sensitivity shown in Figure 5. By 2010, MINOS will have sensitivity to $\sin^2 2\theta_{13}$ down to ~ 0.06, *i.e.* roughly a factor two better than the current limit [11].

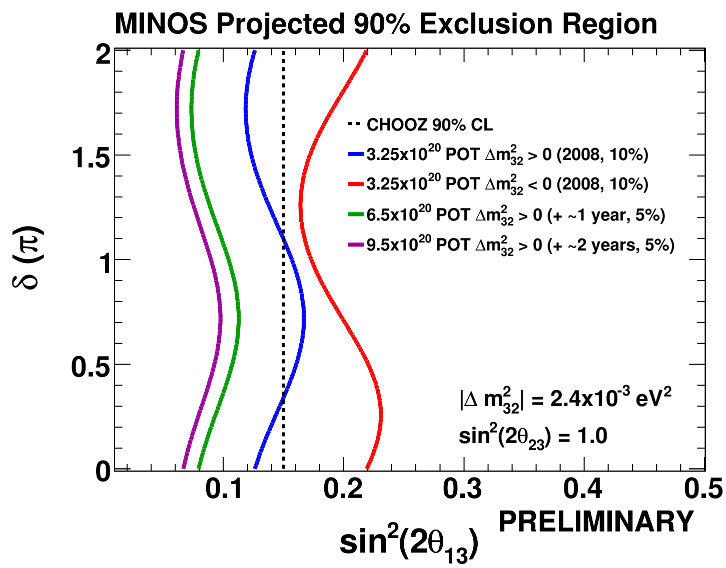

Figure 5: The MINOS projected 90 % C.L. sensitivity to θ_{13} from the search for subdominant $\nu_\mu \to \nu_e$ oscillations. The sensitivities are shown for an exposure of 3.25×10^{20} PoT assuming a 10 % systematic error on the background and for 6.5×10^{20} PoT and 9.5×10^{20} PoT assuming a 5 % background systematic uncertainty. The expected background is derived from the ND data.

In summary, MINOS provides a high statistics test of the neutrino oscillation hypothesis and yields a precise measurement ($\pm 5\,\%$) of $|\Delta m^2_{32}|$. With the final MINOS data the lower bound on θ_{23} may exceed the current limits from SK. MINOS also has sensitivity to θ_{13} beyond the current limits from the CHOOZ experiment.

3.5 OPERA

The OPERA [21] experiment uses the CERN to Gran Sasso (CNGS) beam. The main goal of the experiment is to the observe τ leptons from ν_τ CC interactions arising from $\nu_\mu \rightarrow \nu_\tau$ oscillations. At the CNGS baseline of 732 km the first oscillation minumum occurs at $\sim$1.6 GeV. This is lower than the kinematic threshold, $E_{\nu_\tau} > 3.5$ GeV, for $\nu_\tau + \mathrm{n} \rightarrow \tau^- + \mathrm{p}$. Consequently ν_τ CC interactions can only be observed at energies where the oscillation probability is relatively small. To some extent, this is compensated by the rising ν_τ CC interaction cross section. For this reason the CNGS beam is relatively high energy, with the majority of the neutrino flux between 5 GeV and 25 GeV.

The expected number of ν_τ interactions is relatively small and detecting neutrino induced τ leptons is challenging. The OPERA detector has 150,000 bricks with a layered structure of 1 mm thick lead plates followed by two emulsion layers. The high precision point resolution of the emulsion enables kinked tracks from τ lepton decays to be cleanly identified. Bricks with candidate interactions are identified by scintillator tracking chambers which are located between walls formed from the lead/emulsion bricks. The bricks are robotically removed from the stack for automatic analysis of the emulsion. OPERA commenced its first full physics run in June 2008. For a nominal five year run (at an intensity of 4.5×10^{19} PoT/year) 10 identified ν_τ are expected (assuming the standard oscillation scenario) with a background of approximately 1 event. The OPERA experiment is discussed in more detail elsewhere in these proceedings [22].

4 Future Long Baseline Experiments

The past and current generation LBL neutrino experiments (K2K, MINOS, OPERA) utilise "on-axis" beams, where the beam points towards the far detector. This is the optimal configuration for maximising the neutrino flux. However, the resulting energy spectrum is rather broad as can be seen in Figure 4a. This is non-ideal for the $\nu_\mu \rightarrow \nu_e$ appearance analysis where NC interactions of relatively high energy neutrinos can be a significant (and poorly modelled) background. The next generation of experiments (T2K and NOνA) are designed to improve the sensitivity to $\sin^2 2\theta_{13}$ by an order of magnitude compared to CHOOZ. These experiments employ an "off-axis" beam, where neutrino beam is aligned such that the far detector is a few degrees from the beam axis. Due to the pion decay kinematics producing the beam via $\pi^+ \rightarrow \mu^+\nu_\mu$, the off-axis neutrino beam has a relatively narrow energy spectrum. The peak of the energy spectrum is chosen to correspond to the $\nu_\mu \rightarrow \nu_e$ oscillation maximum, thus maximising the signal. The lack of higher energy neutrinos in the off-axis beam means that the NC background to the ν_e appearance measurement is greatly reduced.

4.1 T2K

The Tokai-to-Kamioka (T2K) experiment will use an intense ν_μ beam produced at the J-PARC facility in Tokai. The main goals of the experiment are to observe ν_e appearance and to measure or set improved lower limits on θ_{23}. First beam is expected in April 2009 with the intensity gradually increasing to the design beam power of 750 kW. First results are anticipated in 2010. T2K employs a 2.5° off-axis beam. The peak energy is approximately 0.6 GeV. The energy spectrum is relatively narrow with a FWHM of approximately 0.3 GeV.

The T2K far detector, located 295 km from the beam, is the 50 kton (22.5 kton fiducial) Super-Kamiokande water Čerenkov detector. T2K has two main near detector systems 280 m from the beam. The on-axis near detector (INGRID) will be used to monitor the beam. It consists of modules with alternating layers of scintillating bars and iron plates. The off-axis detector is more complex. It is divided into three main parts: a tracker, a π^0 detector, and an electromagnetic calorimeter. The tracker consists of three Time Projection Chambers (TPCs) with two fine-grained scintillating bar detectors in between. The main purpose of the tracking detector is to measure the beam flux and energy spectrum and to make measurements of neutrino cross sections and kinematics on order to constrain the far detector expectations. The π^0 detector consists of layers of triangular scintillating bars. In between a number of the layers there is are water targets. The main purpose of the π^0 detector is to study π^0 production in NC interactions; such events form the main background for the ν_e appearance measurement.

Phase I of the T2K experiment assumes a 5 year run with a 0.75 MW beam, corresponding to 5×10^{21} PoT. With this exposure, it is estimated that the uncertainty on $\sin^2 2\theta_{23}$ will be 0.01 and that on $|\Delta m^2_{32}|$ will be $10^{-4}\,\text{eV}^2$. Figure 6a shows the T2K expected sensitivity to θ_{13} (which depends on δ). The limit of the sensitivity is $\sin^2 2\theta_{13} \sim 0.01$ where approximately 10 signal events are expected, compared to the background of approximately 10 electromagnetic shower-like events from NC interactions and 13 events from the residual ν_e component of the beam. Whether T2K can achieve this sensitivity will depend on how well these backgrounds can be constrained by the ND data.

4.2 NOνA

The proposed NOνA project at FNAL is designed to search for ν_e appearance by comparing electron neutrino rates in a large off-axis detector 810 km from Fermilab with the rates in the near detector. In the first stage of the project the NuMI beam would be upgraded to between 400 kW and 700 kW. At the time of writing the schedule for NOνA (and indeed whether the project will go ahead) is unclear. Optimistically one might anticipate first meaningful data in 2013/2014. The planned NOνA detector [24]

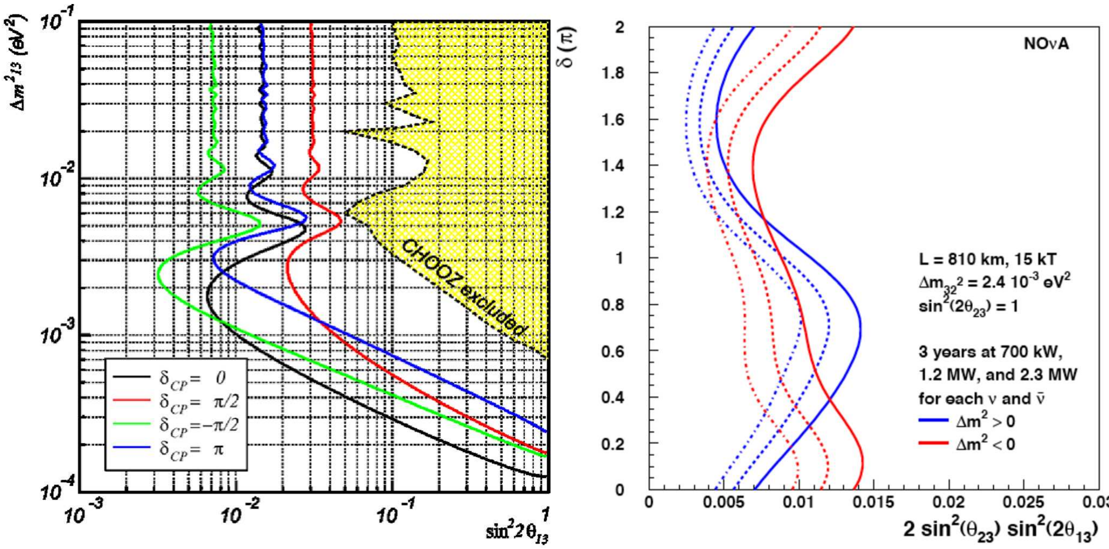

Figure 6: **a)** The expected T2K sensitivity to $\sin^2 2\theta_{13}$ assuming the nominal Phase I run of 5 years at 0.75 MW. The plot is shown for four values of δ. **b)** The expected NOνA sensitivity to $\sin^2 2\theta_{13}$ shown as a function of δ and mass hierarchy. Taken from [25].

consists of approximately 1000 planes made up of 4 cm×6 cm×15.5 m extruded plastic cells containing liquid scintillator. The cells would be read out using avalanche photo-diodes attached to wavelength-shifting fibres. The entire detector would be 15.7 m×15.7 m×67 m in volume, giving a total mass of 15 kton. The totally active detector is optimised for the identification of electro-magnetic showers produced by ν_e CC interactions. The 0.2 kton near detector would be constructed from identical components.

NOνA would be sensitive to θ_{13} down to $\sin^2 2\theta_{13} \sim 0.01$, although a simple interpretation in terms of θ_{13} alone is not possible as the expected ν_e event rates depend not only on θ_{13} but also on the mass hierarchy and the CP phase δ. The current estimated sensitivity is shown in Figure 6b. The final sensitivity will depend on beam intensity for which there are a number of options; upgrade NuMI to $0.4 - 0.7$ MW, Super-NuMI (SNuMI) *i.e.* an upgrade to 1.2 MW or the 2.3 MW beam of Project-X which is currently under discussion.

5 Summary

High intensity long baseline experiments have opened up a new era in the study of neutrino oscillations. The feasibility of LBL neutrino experiments was first demonstrated by K2K. MINOS has provided a precise measurement of $|\Delta m^2_{32}|$ and a high precision test of the oscillation hypothesis. OPERA is currently searching for the first direct evidence of ν_τ appearance in $\nu_\mu \rightarrow \nu_\tau$ oscillations. The next challenge for LBL experiments is the measurement of θ_{13} which will ultimately pave the way to the experimental investigation of CP violation in the lepton sector. The T2K experiment (and hopefully NOνA), along with the next generation of reactor experiments, will be central to the future experimental neutrino physics programme. The next ten years are likely to be every bit as exciting and pivotal for neutrino physics as the last ten years - and that is saying something!

References

[1] Y. Ashie *et al.*, Super-Kamiokande Collaboration, Phys. Rev. Lett. **93**, 101801 (2004).

[2] Y. Ashie *et al.*, Super-Kamiokande Collaboration, Phys. Rev. **D 72**, 112005 (2005).

[3] J. Hosaka *et al.*, Super-Kamiokande Collaboration, Phys. Rev. **D 74**, 032002 (2006).

[4] J. Fukada *et al.*, Super-Kamiokande Collaboration, Phys. Lett. **B 539**, 179 (2002).

[5] J. P. Cravens *et al.*, Super-Kamiokande Collaboration, Phys. Rev. **D 78**, 032002 (2008).

[6] B. Aharmim *et al.*, SNO Collaboration, Phys. Rev. **C 72**, 055502 (2005).

[7] M. Acciarri *et al.*, L3 Collaboration, Phys. Lett. **B 431**, 199 (1998);
P. Abreu *et al.*, Delphi Collaboration, Z. Phys. **C 74**, 577 (1997);
R. Akers *et al.*, OPAL Collaboration, Z. Phys **C 65**, 47 (1995);
D. Buskulic *et al.*, Aleph Collaboration, Phys. Lett. **B 313**, 520 (1993).

[8] Pontecorvo, B., Sov. Phys. JETP **6**, 429 and Zh. Eksp. Teor. Fiz. **33**, 549 (1957).

[9] Maki, Z., Nakagawa, M. and Sakata, S., Progr. Theor. Phys. **28**, 870 (1962).

[10] S. Abe *et al.*, KamLAND Collaboration, Phys. Rev. Lett. **100**, 221803 (2008).

[11] M. Apollonio *et al.*, CHOOZ Collaboration, Phys. Lett. **B 466**, 415 (1999).

[12] H. Meyer for the MIPP Collaboration, J. Phys. Conf. Ser. **69** 012025 (2007).

[13] M. H. Ahn *et al.*, K2K Collaboration, Phys. Rev. **D 74**, 072003 (2006).

[14] Durham Database Group, HEPDATA: Reaction Data Database, http://durpdg.dur.ac.uk/HEPDATA/REAC.

[15] H. Gallagher, Nucl. Phys. B Proc. Suppl. **112**, 188 (2002).

[16] P. Adamson *et al.*, MINOS Collaboration, Phys. Rev. **D 77**, 072002 (2008).

[17] D. Michael *et al.*, MINOS Collaboration, Nucl. Instrum. Meth. **A596**, 190 (2008).

[18] P. Adamson *et al.*, MINOS Collaboration, Phys. Rev. Lett. **101**, 131802 (2008).

[19] V. Barger *et al.*, Phys. Rev. Lett. **82**, 2640 (1999).

[20] G. L. Fogli *et al.*, Phys. Rev. **D 67**, 093006 (2003).

[21] M. Guler *et al.*, CERN/SPSC 2000-028, SPSC/P318, LNGS P25/2000), "An appearance experiment to search for oscillations of the CNGS beam" (2000).

[22] A. Longhin, these proceedings.

[23] Y. Itow *et al.*, T2K Collaboration, KEK-REPORT-2001-4, ICRR-REPORT-477-2001-7, TRI-PP-01-05, hep-ex/0106019, (2001).

[24] NOνA, NuMI Off-Axis ν_e Appearance Experiment, TDR, October 2007; http://www-nova.fnal.gov/nova_cd2_review/tdr_oct_23/tdr.htm.

[25] G. Feldman, "The NOνA Experiment", talk at the P5 eeting, SLAC, February 2008; http://www-group.slac.stanford.edu/ppa/Reviews/p5/.